Numerical simulation of current noise caused by potential fluctuation in nanowire FET with an oxide trap

Yuki Furubayashi, Matsuto Ogawa, and Satofumi Souma†
Department of Electrical and Electronic Engineering, Kobe University, Kobe 657-8501, Japan
†email: ssouma@harbor.kobe-u.ac.jp

***Abstract*—We present a theoretical study on the temporal current fluctuation in nanowire FET caused by the presence of a single gate oxide trap through the Coulomb interaction. Our calculations based on the scattering theoretical formulation of the current noise showed that the presence of the trap level in the gate insulator gives rise to the enhancement of the noise at a specific gate voltage. The peak position of the noise is related to the capacitive coupling strengths of the trap to the channel and the gate electrode, suggesting that the current noise can be used to measure such physical quantities.**

I. Introduction

Recent rapid development of semiconductor technology has been mainly achieved by the miniaturization of the silicon MOSFET down to nanoscale. Such aggressive down-scaling, however, has been causing various drawbacks such as the leakage current and the variation of the threshold voltage due to the non-uniformity of the discrete dopants. Moreover, it has been argued recently that in the sub 22 nm process the random telegraph noise (RTN) may influence more seriously the device performance. The origin of RTN has been attributed to the trapping and detrapping of the carriers by various lattice vacancies in the gate oxide [1], [2], [3], [4]. Such trapping and detrapping process cause the temporal fluctuation of the current, degrading the device performance.

While the noise degrades the device performance in general, it sometimes plays informative role in understanding the microscopic properties of the system. One of the well known such examples is the detection of the fractional charge through the shot noise in the fractional quantum Hall system. It should also be of importance to explore the fundamental aspect of the current noise in nanoscale MOSFET. With such motivation, the purpose of this paper is to clarify theoretically how the presence of a single trap level in the gate oxide of nanowire (NW) FET induces the temporal current noise through the Coulomb interaction.

II. Theoretical method

In this section we introduce the general theoretical framework to estimate the current noise caused by the temporal potential fluctuation. We consider a multi-terminal conductor, where each αth terminal (lead) is single moded and is connected to an electron reservoir specified by the Fermi distribution function $f_\alpha(E)$ with the Fermi energy μ_α. Electrons in the scattering region are assumed to feel the time-fluctuating potential $\delta V(\boldsymbol{r},t)$ caused by the fluctuation of the charge density in the conductor in addition to the static potential $V_0(\boldsymbol{r})$, so that the total potential is given by

$$V(\boldsymbol{r},t) = V_0(\boldsymbol{r}) + \delta V(\boldsymbol{r},t). \qquad (1)$$

In the absence of the time-fluctuating potential $\delta V(\boldsymbol{r},t)$, the current in the αth lead is simply evaluated as

$$I_\alpha^{(0)} = \frac{q}{h}\int dE \sum_{\beta}^{N_{\mathrm{term}}} f_\beta(E)\,\mathrm{Tr}[A_{\beta\beta}(\alpha,E,E)], \qquad (2)$$

where N_{term} is the number of terminals (leads),

$$A_{\beta\beta}(\alpha,E,E) = 1_\beta\delta_{\alpha\beta} - s^\dagger_{\alpha\beta}(E)\,s_{\alpha\beta}(E), \qquad (3)$$

with $s_{\alpha\beta}$ being the spin-resolved scattering matrix relating the injection from the βth leads to the ejection to the αth lead, Tr denoting the trace over spin space. The presence of time-fluctuating potential $\delta V(\boldsymbol{r},t)$ is, if it is small enough, considered as causing the time-fluctuation of the current in the linear order of the potential fluctuation as

$$\delta I_\alpha(t) = \int d^3\boldsymbol{r}\,\frac{\delta I_\alpha^{(0)}}{\delta V(\boldsymbol{r})}\delta V(\boldsymbol{r},t), \qquad (4)$$

where $\delta I_\alpha^{(0)}/\delta V(\boldsymbol{r})$ is the functional derivative of the current $I_\alpha^{(0)}$ in Eq. (2) with respect to the potential distribution $V(\boldsymbol{r})$. We note that, if the potential fluctuation $\delta V(\boldsymbol{r},t)$ is time-averaged to zero (it is the case in our present problem), the time-averaging of the full time-dependent current $I_\alpha(t) \equiv I_\alpha^{(0)} + \delta I_\alpha(t)$ results in the current without the potential fluctuation so that $\overline{I_\alpha(t)} = I_\alpha^{(0)}$. Therefore we can replace $I_\alpha^{(0)}$ in Eq. (4) by $\overline{I_\alpha(t)}$.

As we mentioned above, the origin of the time-fluctuating potential is the fluctuation of the charge distribution in the conductor. Therefore it is expressed as $\delta V(\boldsymbol{r},t) = q\delta\phi(\boldsymbol{r},t)$ with $\delta\phi(\boldsymbol{r},t)$ being the electrostatic potential fluctuation ($q=-|e|$ is the charge of an electron), where $\delta\phi(\boldsymbol{r},t)$ is related to the carrier density fluctuation $\delta n(\boldsymbol{r},t)$ by the Poisson's equation as

$$\nabla\varepsilon(\boldsymbol{r})\nabla\delta\phi(\boldsymbol{r},t) = -q\delta n(\boldsymbol{r},t), \qquad (5)$$

where $\varepsilon(\boldsymbol{r})$ is the position dependent dielectric permittivity. In order treat the temporal carrier density fluctuation systematically, we employ the second-quantization formalism. The

978-1-4799-5288-5/14/$31.00

electron density operator corresponding to electrons *injected* from all the electrodes is given by

$$\hat{n}_{\text{inj}}(\boldsymbol{r},t) = \sum_{\alpha,\beta}\sum_{\sigma,\sigma'}\int dE_\alpha \int dE_\beta \nu_{\alpha\sigma,\beta\sigma'}(\boldsymbol{r},E_\alpha,E_\beta) \times \hat{a}^\dagger_{\alpha\sigma}(E_\alpha)\,\hat{a}_{\beta\sigma'}(E_\beta)\,e^{-i(E_\beta-E_\alpha)t/\hbar}, \tag{6}$$

where we have introduced the function $\nu_{\alpha\sigma,\beta\sigma'}(\boldsymbol{r},E_\alpha,E_\beta) = (1/h)\psi^*_{\alpha\sigma}(\boldsymbol{r},E_\alpha)\psi_{\beta\sigma'}(\boldsymbol{r},E_\beta)/\sqrt{v_\alpha(E_\alpha)v_\beta(E_\beta)}$ expressing the on- and off-diagonal elements of the the local density of states with $\psi_{\alpha\sigma}(\boldsymbol{r},E_\alpha)$ being the scattering state for an spin-σ electron incident from the αth lead with energy E_α and $v_\alpha(E_\alpha)$ the corresponding group velocity in the αth (spin-degenerate) lead, $\hat{a}^\dagger_{\alpha\sigma}$ ($\hat{a}_{\alpha\sigma}$) is the second-quantized operator to create (annihilate) an electron incident from the αth lead. In this second-quantized representation, the electron density fluctuation is also an operator, given as

$$\delta\hat{n}_{\text{inj}}(\boldsymbol{r},t) \equiv \hat{n}_{\text{inj}}(\boldsymbol{r},t) - \langle\hat{n}_{\text{inj}}(\boldsymbol{r},t)\rangle, \tag{7}$$

where $\langle\cdots\rangle$ denotes the nonequilibrium quantum statistical expectation value in the occupation number space [5]. This electron density fluctuation causes an electrostatic potential fluctuation through the Poisson's equation (5). However here we note that now both sides in Eq. (5) are operators. In response to the the electrostatic potential fluctuation $\delta\hat{\phi}(\boldsymbol{r},t)$, there should arise an *induced* electron density fluctuation, which can be written in general as

$$\delta\hat{n}_{\text{ind}}(\boldsymbol{r},t) = -\int d^3\boldsymbol{r}'\Pi(\boldsymbol{r},\boldsymbol{r}';t,t')\,q\delta\hat{\phi}(\boldsymbol{r}',t'), \tag{8}$$

where $\Pi(\boldsymbol{r},\boldsymbol{r}';t,t')$ is response function, and is an unknown function at this stage. Equation (7) is Fourier transformed with respect to time to obtain

$$\delta\hat{n}_{\text{inj}}(\boldsymbol{r},\omega) = \hbar\sum_{\alpha,\beta,\sigma,\sigma'}\int dE\nu_{\alpha\sigma,\beta\sigma'}(\boldsymbol{r},E,E+\hbar\omega) \times\left\{\hat{a}^\dagger_{\alpha\sigma}(E)\,\hat{a}_{\beta\sigma'}(E+\hbar\omega) - \left\langle\hat{a}^\dagger_{\alpha\sigma}(E)\,\hat{a}_{\beta\sigma'}(E+\hbar\omega)\right\rangle\right\}. \tag{9}$$

Electron density fluctuation Eq. (8) induced by the potential fluctuation is also Fourier transformed as

$$\delta\hat{n}_{\text{ind}}(\boldsymbol{r},\omega) = -\int d^3\boldsymbol{r}'\tilde{\Pi}(\boldsymbol{r},\boldsymbol{r}';\omega)\,q\delta\hat{\phi}(\boldsymbol{r}',\omega). \tag{10}$$

In our present study, we assume the zero frequency limit and employ the linear response treatment for the response function [6],

$$\tilde{\Pi}(\boldsymbol{r},\boldsymbol{r}') = -\sum_\alpha\int dE\frac{\delta\nu_\alpha(\boldsymbol{r},E)}{\delta V(\boldsymbol{r}')}f(E-\mu_\alpha), \tag{11}$$

where $\nu_\alpha(\boldsymbol{r},E) = \nu_{\alpha\alpha}(\boldsymbol{r},E,E)$ is the partial density of states for electrons incident from the αth lead. The electrostatic potential fluctuation is then determined as the one induced by the summation of these two electron density fluctuations through the Poisson's equation as

$$\nabla\varepsilon(\boldsymbol{r})\nabla\delta\hat{\phi}(\boldsymbol{r},\omega) = -q\left\{\delta\hat{n}_{\text{inj}}(\boldsymbol{r},\omega) + \delta\hat{n}_{\text{ind}}(\boldsymbol{r},\omega)\right\}. \tag{12}$$

We note that the solution to this equation (i.e., $\delta\hat{\phi}(\boldsymbol{r},\omega)$) is required to evaluate $\delta\hat{n}_{\text{ind}}(\boldsymbol{r},\omega)$ in second term through Eq. (10), meaning that Eq. (12) is a nonlinear (or self-consistent) equation. Nevertheless, the formal solution to Eq. (12) can be written as

$$\delta\hat{\phi}(\boldsymbol{r},\omega) = q\int d^3\boldsymbol{r}'g(\boldsymbol{r},\boldsymbol{r}')\,\delta\hat{n}_{\text{inj}}(\boldsymbol{r}',\omega), \tag{13}$$

where $g(\boldsymbol{r},\boldsymbol{r}')$ is the Green's function satisfying the equation

$$\int d^3\boldsymbol{r}'\left\{-\delta(\boldsymbol{r}-\boldsymbol{r}')\nabla'^2 + e^2\tilde{\Pi}(\boldsymbol{r},\boldsymbol{r}';\omega)\right\}g(\boldsymbol{r},\boldsymbol{r}') = \delta(\boldsymbol{r}-\boldsymbol{r_0}). \tag{14}$$

Once the potential fluctuation is obtained by Eq. (13), the current induced by the potential fluctuation is obtained by using Eq. (4). However, since the potential fluctuation in Eq. (13) is a second-quantized operator, the current in Eq. (4) has to be generalized to the second-quantized expression. First, the Fourier transformed current operator (without the fluctuation current) is

$$\hat{I}^{(0)}_\alpha(\omega) = q\int dE\sum_{\gamma,\delta,\sigma,\sigma'}\hat{a}^\dagger_{\gamma\sigma}(E)\,A_{\gamma\sigma,\delta\sigma'}(\alpha,E,E+\hbar\omega) \times\hat{a}_{\delta\sigma'}(E+\hbar\omega), \tag{15}$$

with $A_{\gamma\sigma,\delta\sigma'}(\alpha,E,E+\hbar\omega)$ being the spin σ-σ' element of

$$A_{\gamma\delta}(\alpha,E,E+\hbar\omega) = 1_\alpha\delta_{\alpha\gamma}\delta_{\alpha\delta} - s^\dagger_{\alpha\gamma}(E)\,s_{\alpha\delta}(E+\hbar\omega). \tag{16}$$

The second-quantized operator corresponding to the current caused by the potential fluctuation is given similarly to Eq. (4)

$$\delta\hat{I}_\alpha(\omega) = \int d^3\boldsymbol{r}\frac{\delta\left\langle\hat{I}_\alpha(\omega)\right\rangle}{\delta V(\boldsymbol{r})}q\delta\hat{\phi}(\boldsymbol{r},\omega), \tag{17}$$

where we have introduced the full Fourier transformed current operator $\hat{I}_\alpha(\omega) \equiv \hat{I}^{(0)}_\alpha(\omega) + \delta\hat{I}_\alpha(\omega)$ and used the fact that its nonequilibrium quantum statistical expectation value of is $\left\langle\hat{I}_\alpha(\omega)\right\rangle = \left\langle\hat{I}^{(0)}_\alpha(\omega)\right\rangle$ since $\left\langle\delta\hat{\phi}(\boldsymbol{r},\omega)\right\rangle = 0$. The actual current fluctuation operator needed to evaluate the temporal current noise is

$$\begin{aligned}\Delta\hat{I}_\alpha(\omega) &= \hat{I}_\alpha(\omega) - \left\langle\hat{I}_\alpha(\omega)\right\rangle \\ &= \hat{I}^{(0)}_\alpha(\omega) + \delta\hat{I}_\alpha(\omega) - \left\langle\hat{I}^{(0)}_\alpha(\omega)\right\rangle.\end{aligned} \tag{18}$$

By substituting Eqs. (13) and (15) into Eq. (17), we obtain

$$\delta\hat{I}_\alpha(\omega) = q\int dE\sum_{\gamma,\delta,\sigma,\sigma'}K_{\gamma\sigma,\delta\sigma'}(\alpha,E,E+\hbar\omega) \times\left\{\hat{a}^\dagger_{\gamma\sigma}(E)\,\hat{a}_{\delta\sigma'}(E+\hbar\omega) - \left\langle\hat{a}^\dagger_\gamma(E)\,\hat{a}_\delta(E+\hbar\omega)\right\rangle\right\}, \tag{19}$$

where

$$K_{\gamma\sigma,\delta\sigma'}(\alpha,E,E+\hbar\omega) = q\hbar\int d^3\boldsymbol{r}\frac{\delta\left\langle\hat{I}_\alpha\right\rangle}{\delta V(\boldsymbol{r})}\int d^3\boldsymbol{r}'g(\boldsymbol{r},\boldsymbol{r}') \times\nu_{\gamma\sigma,\delta\sigma'}(\boldsymbol{r},E,E+\hbar\omega) \tag{20}$$

is the current fluctuation kernel due to the potential fluctuation. Therefore the operator for the full current fluctuation is calculated by

$$\Delta \hat{I}_\alpha(\omega) = q \int dE \sum_{\gamma,\delta,\sigma,\sigma'} \times \left\{ A_{\gamma\sigma,\delta\sigma'}(\alpha, E, E+\hbar\omega) + K_{\gamma\sigma,\delta\sigma'}(\alpha, E, E+\hbar\omega) \right\} \times \left\{ \hat{a}^\dagger_{\gamma\sigma}(E)\, \hat{a}_{\delta\sigma'}(E+\hbar\omega) - \left\langle \hat{a}^\dagger_{\gamma\sigma}(E)\, \hat{a}_{\delta\sigma'}(E+\hbar\omega) \right\rangle \right\}. \tag{21}$$

Following the same procedure as in Ref. [5], current-current fluctuation spectrum $S_{\alpha\beta}(\omega)$ is introduced by the relation

$$\frac{1}{2}\left[\left\langle \Delta \hat{I}_\alpha(\omega)\, \Delta \hat{I}_\beta(\omega') \right\rangle + \left\langle \Delta \hat{I}_\beta(\omega')\, \Delta \hat{I}_\alpha(\omega) \right\rangle \right] = 2\pi S_{\alpha\beta}(\omega)\, \delta(\omega + \omega'). \tag{22}$$

By substituting Eq. (21) into this equation, we obtain

$$S_{\alpha\beta}(\omega) = \frac{e^2}{\hbar} \int dE \sum_{\gamma\delta} \mathrm{Tr}\left[B_{\gamma\delta}(E, E+\hbar\omega) \right] \times F_{\gamma\delta}(E, E+\hbar\omega), \tag{23}$$

where Tr denotes the trace over spin space,

$$F_{\gamma\delta}(E, E+\hbar\omega) = f_\gamma(E)\left\{1 - f_\delta(E+\hbar\omega)\right\} + f_\delta(E+\hbar\omega)\left\{1 - f_\gamma(E)\right\}, \tag{24}$$

and

$$B_{\gamma\delta}(E, E+\hbar\omega) = \sum_{i=1}^{4} B_{\gamma\delta,i}, \tag{25}$$

$$B_{\gamma\delta,1} = A_{\gamma\delta}(\alpha, E, E+\hbar\omega)\, A_{\delta\gamma}(\beta, E+\hbar\omega, E) \tag{26}$$

$$B_{\gamma\delta,2} = A_{\gamma\delta}(\alpha, E, E+\hbar\omega)\, K_{\delta\gamma}(\beta, E+\hbar\omega, E) \tag{27}$$

$$B_{\gamma\delta,3} = K_{\gamma\delta}(\alpha, E, E+\hbar\omega)\, A_{\delta\gamma}(\beta, E+\hbar\omega, E) \tag{28}$$

$$B_{\gamma\delta,4} = K_{\gamma\delta}(\alpha, E, E+\hbar\omega)\, K_{\delta\gamma}(\beta, E+\hbar\omega, E). \tag{29}$$

Equation (23) is a central equation in our numerical calculation. In the absence of the potential fluctuation induced term (i.e., Eq. (20)), Eq. (23) is reduced to the conventional (shot+thermal) noise expression in Ref. [5], [6], [7]. In our actual calculations presented below, we evaluate the zero-frequency limit of the noise Eq. (23) with taking into account the contributions of only the conventional noise term (Eq. (26)) and Coulomb noise term (Eq. (29)).

III. Numerical Results

As a representative example, we consider GaAs NW-FETs with a single trap level in the gate oxide as schematically shown in Fig. 1. Here the NW is assumed to be single-moded, and has been modeled by the one-dimensional tight-binding lattice (within the finite-difference approximation scheme) with the hopping energy $t_{\mathrm{hop}} = \hbar^2/2m^* a_0^2$, where $m^* = 0.067 m_0$ is the effective mass of an conduction band electron (m_0 is the free electron mass) and $a_0 = 1$ nm is the finite-difference lattice spacing. Room temperature 300 K is assumed throughout this paper. A single trap level in the gate oxide is assumed to be coupled electronically with the NW at its

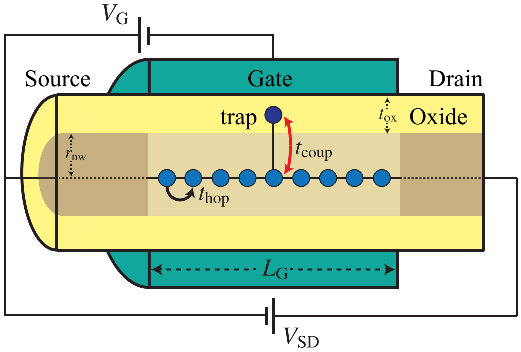

Fig. 1. Schematic illustration of the GaAs NW-FET with a single oxide trap located at the middle point of the gate along the current direction. Gate length L_{G} of $5 \sim 9$ nm is assumed in the calculation of electronic transport, while the radius of nanowire $r_{\mathrm{nw}} = 5$ nm and the gate oxide thickness $t_{\mathrm{ox}} = 1$ nm are used to calculate the gate capacitance. Source and drain regions are assumed to be n-type to allow the downward band-shifting by 0.285 eV with respect to the intrinsic channel region. In our calculations, applied gate positive voltage is simply assumed to be equal to the downward shift of the potential in t

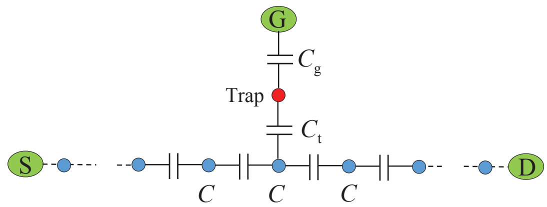

Fig. 2. Schematic illustration of the capacitance network model used to solve Eq. (14) numerically. Three effective capacitance values are estimated assuming the cylindrical NW geometry as $C = 9.11$ aF, $C_{\mathrm{g}} = 0.203$ aF, and $C_{\mathrm{t}} = 2.34$ aF.

middle position with the coupling energy $t_{\mathrm{coup}} = 0.01 \times t_{\mathrm{hop}}$. Electrostatic Green's function in Eq. (14) is also solved numerically within the finite difference scheme with the help of the phenomenological capacitance model illustrated in Fig. 2. In Fig. 3 we show the I_{D}-V_{G} characteristics computed by using Eq. (2). In the calculated result we can see that the typical I_{D}-V_{G} characteristics of MOSFETs is obtained even in the presence of the trap in the gate oxide.

Next we consider the current noise calculated by using Eq. (23) in the presence of potential fluctuation due to the oxide trap. In Fig. 4 we plotted the Coulomb noise and conventional noise (shot noise plus thermal noise) separately as a function of the gate voltage. Here we see that the Coulomb noise exhibits a sharp peak and exceeds the conventional noise at around a specific gate voltage. Moreover our calculations show that the shorter L_{G} gives bigger noise at the peak position, meaning the significance of the Coulomb noise in the further miniaturization. In order to clarify the physical origin which determines the peak position, in Fig. 5 we show the gate voltage dependence of the intra-trap electrostatic response function $\Pi(\boldsymbol{r}, \boldsymbol{r})$ (Eq. (11)) at the oxide trap position together with the corresponding electrostatic Green's function $g(\boldsymbol{r}, \boldsymbol{r})$ (Eq. (14)). By comparing Figs. 4 and 5, we can understand

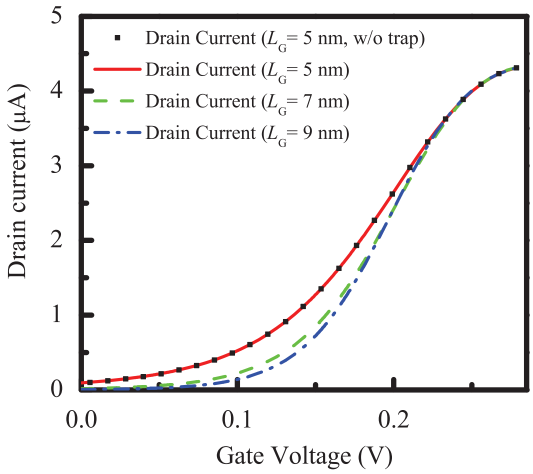

Fig. 3. I_D-V_G characteristics for $L_G = 5, 7, 9$ nm in the absence and the presence of the trap site. Fermi energy is positioned at 0.114 eV above the conduction band bottom in the source electrodes, while the trap site energy is assumed to be 0.171 eV above the band bottom in the electrodes at the zero gate voltage. Drain voltage 0.057 V is assumed. Trap level is shifted lower in energy simultaneously with the channel potential by increasing the gate voltage.

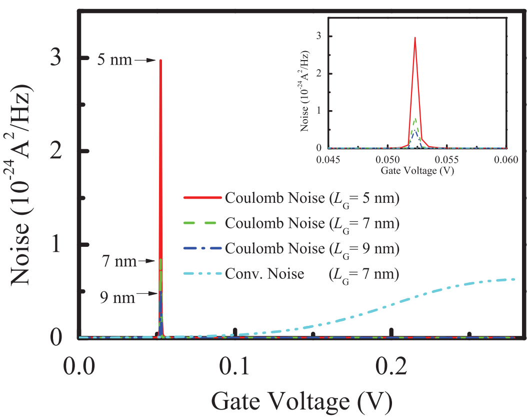

Fig. 4. Noise-V_G characteristics for $L_G = 5, 7, 9$ nm (with the same conditions as in Fig. 3. Peak heights for three cases are indicated by arrows. The inset is the magnified view around the noise peak in the main panel.

that the Coulomb noise exhibits a peak when the intra-trap electrostatic response function (negatively valued as shown in Fig. 5) matches the minus of the sum of C_t and C_g, which are the trap-NW and trap-gate capacitances, respectively. The electrostatic intra-trap Green's function is enhanced around such matching point, giving rise to the peak in the Coulomb noise through Eq. (20). Such enhancement of noise is similarly observed in resonant tunneling diode structures [8], [9].

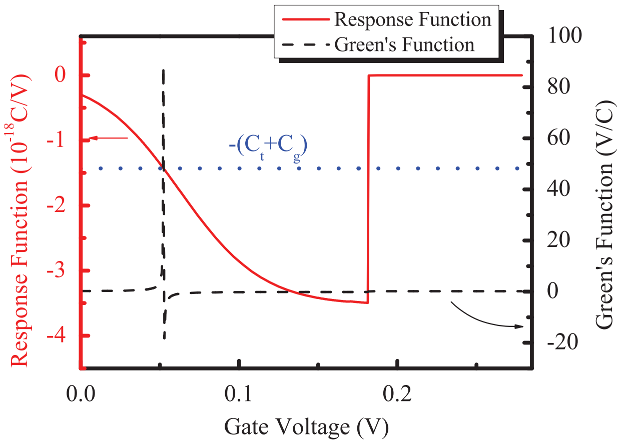

Fig. 5. Intra-trap electrostatic responsive function (black trace, left axis) and the intra-trap electrostatic Green's function (blue trace, right axis) are plotted as a function of V_G.

IV. Conclusion

We have presented a theoretical study on the temporal current fluctuation in nanowire FET caused by the presence of a single gate oxide trap through the Coulomb interaction. By generalizing the conventional scattering theoretical formulation of the current noise to include the potential fluctuation noise, we have obtained the closed expression for such Coulomb noise. Our calculations based on the derived noise expression have shown that the presence of the trap level gives rise to the enhancement of the noise at a specific gate voltage. The peak position of the noise is related to the capacitive coupling strengths of the trap to the channel and the gate electrode, suggesting that the current noise can be used to measure such physical quantities.

References

[1] H. F. Chiu, S. L. Wu, Y. S. Chang, S. J. Chang, J. F. Chen, S. C. Tsai, C. H. Hsu, C. M. Lai, C. W. Hsu, and O. Cheng, "Impact of oxygen annealing on high-k gate stack defects characterized by random telegraph noise," Appl. Phys. Lett. **101**, 122105 (2012).

[2] A. N. Nazarov, I. Ferain, N. D. Akhavan, P. Razavi, R. Yu, and J. P. Colinge, "Random telegraph-signal noise in junctionless transistors," Appl. Phys. Lett. **98**. 092111 (2011).

[3] H. H. Mueller and M. Schulz, "Random telegraph signal: An atomic probe of the local current in field-effect transistors," J. Appl. Phys. **83**.1734 (1998).

[4] J. Salfi, N. Paradiso, S. Roddaro, S. Heun, S. V. Nair, I. G. Savelyev, M. Blumin, F. Beltram, H. E. Ruda. "Probing the Gate-Voltage-Dependent Surface Potential of Individual InAs Nanowires Using Random Telegraph Signals," ACS Nano **5**, 2191 (2011).

[5] M. Büttiker, "Scattering theory of current and intensity noise correlations in conductors and wave guides," Phys. Rev. B **46**, 19 (1992).

[6] M. Büttiker, "Dynamic conductance and quantim noise in mesoscopic conductors," J. Math. Phys. **37**, 10 (1996).

[7] Y. M. Blanter, M. Büttiker "Shot Noise In Mesoscopic Conductors," Physics Reports **336**, 1 (2000).

[8] D. Li, L. Zhang, F. Xu, and J. Wang, "Enhancement of shot noise due to the fluctuation of Coulomb interaction," Phys. Rev. B **85** 165402 (2012).

[9] G. Iannaccone, G. Lombardi, M. Macucci, and B. Pellegrini, "Enhanced Shot Noise in Resonant Tunneling: Theory and Experiment," Phys. Rev. Lett **80** 1054 (1998).